symmetry

MDPI

Article

A Method for Calculating the Sign and Degree of Chirality of Supercoiled Protein Structures

Aleksey Lutsenko, Alla Sidorova, Denis Shpigun, Ekaterina Belova and Vsevolod Tverdislov *

Faculty of Physics, Lomonosov Moscow State University, Leninskie Gory 1-2, 119234 Moscow, Russia
* Correspondence: tverdislov@mail.ru

Abstract: Chirality plays an important role in studies of natural protein structures. Therefore, much attention is paid to solving the problems associated with the development of criteria and methods for assessing the chirality of biomolecules. In this paper, a new method for calculating the sign and degree of chirality of superhelices is proposed. The method makes it possible to characterize the chirality sign and to quantify coiled-coils and collagen superhelices. The degree of chirality is understood as a value indicating the intensity of twisting of individual helices around the axis of the superhelix. The calculation requires information about the relative spatial arrangement of the alpha carbon of the amino acid residues of the helices that make up the superhelix. The use of a small amount of raw data makes the method easy to apply, and the validity of the results of this study is confirmed through the analysis of real protein structures.

Keywords: chirality; proteins; secondary structure; superhelix; coiled-coil; collagen

Citation: Lutsenko, A.; Sidorova, A.; Shpigun, D.; Belova, E.; Tverdislov, V. A Method for Calculating the Sign and Degree of Chirality of Supercoiled Protein Structures. *Symmetry* **2023**, *15*, 2051. https://doi.org/10.3390/sym15112051

Academic Editors: John H. Graham and Chris Bishop

Received: 29 July 2023
Revised: 22 October 2023
Accepted: 9 November 2023
Published: 12 November 2023

1. Introduction

Chirality is a geometric property of physical objects [1] and is one of the most important properties of molecular and biological systems; it is therefore a subject of active basic research. Much attention is paid to solving the problems associated with the development of criteria and methods for assessing the chirality of biomolecules as well as to revealing the relationships between their internal structures and biological functions [2–13]. Chirality can dramatically affect the processes of self-organization related to the formation of macromolecular structures [13,14]. One of the fundamental aspects of this effect is a systemic relation between the structural hierarchy and the alternation of the chirality sign at each level of biomacromolecule structure formation. The structures of proteins and nucleic acids generally have a certain fixed chirality within one class of molecules and one structural level, whereas in transitions between neighboring structural levels, the chirality sign most often reverses. For example, the helical structures of proteins have a tendency to retain one chirality sign: α-helices are right-handed in the vast majority, whereas polyproline helices are left-handed. Supersecondary elements formed from them have the opposite chirality signs. Coiled-coils formed from α-helices are left-handed, and collagen superhelices formed from polyproline helices are right-handed.

Coiled-coils are structural motifs that are formed from several α-helices. Most often they consist of two or three α-helices, but there can be more. For example, there are constructions of six and seven α-helices [15]. The constituent helices in this construction can be parallel and antiparallel [16]. Domains with coiled-coils occur in approximately 10% of all proteins [17].

Superhelices are key elements of many proteins, allowing them to perform their functions in a variety of biological processes. For example, superhelical domains of proteins are involved in transcription, membrane fusion, muscle functioning, cell division, chemotaxis mechanisms, and the interaction of pathogens with host cells. They also play a crucial

role in the cytoskeleton and extracellular matrix [18] and are involved in the folding process [19] and DNA repair [20]. They can be used as targets for pharmacological applications, including drug delivery systems [21,22].

In the classical coiled-coil superhelix, the amino acid sequence is divided into heptads—sequences of seven amino acid residues. The mutual arrangement of residues relative to each other is identical in each heptad [23]. The distribution of residues into heptads is achieved due to the fact that in a superhelix, each α-helix is slightly rotated with respect to its natural position. Although an individual α-helix has approximately 3.6 amino acid residues per turn, in the coiled-coil structure, there is exactly one heptad (7 residues) per two turns, and 3.5 residues per one turn, respectively [16]. This leads to the fact that the mutual positions of corresponding residues in different helices of the superhelix remain unchanged throughout the superhelix. Heptad positions are denoted by the letters *a*, *b*, *c*, *d*, *e*, *f*, and *g*. Positions *a* and *d* are usually occupied by hydrophobic residues that form the core of the superhelix with "knobs into holes" packing [23,24]. Superhelices consisting of three or more α-helices often have stabilizing ionic interactions between the polar amino acid residues at positions *e* and *g* [25].

Occasionally, heptadic sequence abnormalities occur in superhelices. The most common type of heterogeneity is the inclusion of additional amino acid residues. The inclusion of an extra three residues is called a stammer, and the inclusion of four is called a stutter [26]. Because there are 3.5 amino acid residues per turn in the heptad, adding a stammer to the heptad causes the α-helix to unwind slightly to complete the inclusion to a full turn, increasing its left-handed twist. The addition of a stutter, on the other hand, causes the helix to flatten, which increases its right-handed twist. The inclusion of a stammer results in a local decade motif, that is, ten residues distributed over three turns [27]. The inclusion of a stutter results in a local hendecade motif, that is, eleven residues distributed over three turns [27]. Accordingly, the addition of a stammer leads to an overall increase in the left-handedness of the superhelix, and the addition of a stutter leads to an increase in the right-handedness of the superhelix. Schmidt et al. presented a method for automatic detection and classification of inclusions based on the three-dimensional structure of the protein [28]. A theory was developed that predicts changes in the structure of the whole superhelix depending on the length of the helix in which the inclusion is located—the accommodation length. On the basis of an analysis of the experimental structures, the authors found that a short accommodation length causes greater changes in the helix angles and increased structural asymmetry compared with a long accommodation length.

Another common type of superhelix is a collagen superhelix. Collagen is a common structural protein in all animals. In humans, it constitutes approximately 30% by weight of all proteins and is a major component of the extracellular matrix. In vertebrates, 28 different types of collagen have been identified, consisting of at least 46 different polypeptide chains [29]. Collagen proteins are usually divided into two structurally different groups—fibrillar and non-fibrillar collagen [30]. Fibrillar collagen makes up about 90% of all collagen present in the human body.

Non-fibrillar collagen is very diverse in structures, arrangements, and properties. Although it makes up only about 10% of all collagen in the human body, it is a vital part of many organs [31]. However, because of the reduced proportion of superhelix structures in non-fibrillar collagen, it will not be discussed further in this work. Conversely, fibrillar collagen is a right-handed superhelix consisting of three left-handed polyproline helices. The collagen superhelix is stabilized by hydrogen bonds between the individual helices [29].

Thus, the following conclusions can be drawn. Firstly, each type of structure considered has a pronounced tendency to homochirality. The α-helices have a right twist, while the polyproline helices have a left twist. Coiled-coils are left-handed, and collagen superhelices are right-handed. Secondly, superhelical structures have a different sign of chirality than the helices of which they are composed. We believe that this pattern reflects some significant physical regularities that lead to complex protein structures and their constituent elements having different signs of chirality. Perhaps these patterns can be

traced at other hierarchical levels. However, it seems important to us to back up these observations with mathematical calculations.

The first mathematical description of coiled-coil structures was made by F. Crick [23,32]. He used the radii of α-helices as well as the radius and pitch of the superhelix. It is important to note that in this model, the twisting directions of the individual helices and the whole superhelix are different. Crick's parametric equations were refined in [33] so that they can also be used to describe superhelices with heptadic repetition violations. This allowed the possibility of heptadic motifs in the structure of the superhelices to be taken into account. In [34], it was proposed to relate the pitch and radius of a superhelix to the variation in the twist angle and shift along the axis of the superhelix per amino acid, which allowed the calculation of this important parameter for the F. Crick model. In [35], it was proposed to calculate the pitch of the double-helix superhelix through the Cartesian vector coordinates of the middle atomic positions of the N- and C-chain backbone atoms. The superhelix axis was defined as the line joining the midpoints of the sections passed between the corresponding atoms of both chains. Thus, different authors [23,32–35] provided complementary models of the coiled-coil superhelix, describing them from the structural point of view as a class of protein elements. However, the presented descriptions did not allow determination of the chirality of a particular structure, and they were mainly focused on the consideration of a model idealized object.

A completely different approach was used in [8]. The authors proposed to determine the chirality of the "surface curve" for each α-helix. The surface curve is considered to be the line in the middle between the curve that connects the heptad residues at the *a* positions and the curve that connects the heptad residues at the *d* positions of the individual α-helices. The periodicity of the helix is taken into account in the model, as is the angle between neighboring residues, which is taken as 100°, and the shift along the axis per amino acid, which is taken as 1.5 Å. In the calculation, the surface curves for the different α-helices included in the superhelix were shown to be left-handed. However, the authors noted that the chirality sign of the surface curve did not necessarily coincide with the chirality sign of the entire superhelix. Thus, this approach also does not provide an objective estimate of the chirality signs of superhelical structures.

Previously, we proposed a method for estimating the chirality signs of protein superhelices [36]. In order to use the method, it is sufficient to know only the mutual arrangement of α-carbons in the chain. The direction of the angles between the axis of the superhelix and the axes of the component helices indicates the direction of twist of the entire superhelix. If α-helices are deflected from the superhelix axis clockwise, then the superhelix is left-handed; if counterclockwise, then it is right-handed. The direction of the twist angle is determined using the properties of vector and scalar products. The chirality sign of the superhelix is calculated by averaging the cosines of the corresponding angles for all the helices forming the superhelix. Calculations using this method showed that coiled-coils are left-handed superhelices and collagen superhelices are right-handed. However, although this method has been shown to be very effective, it has some disadvantages. One of them is that the chirality sign is calculated for only a small terminal fragment of a superhelix; consequently, the remaining structure is not taken into account at all. However, no conclusions can be drawn from the angle about the degree of chirality of the superhelix, and the method is not applicable for this purpose. Therefore, it was decided to develop a new method taking into account these important aspects.

2. Materials and Methods

Here we propose a new method to estimate the chirality sign and degree of protein superhelices such as coiled-coils and collagen superhelices. In this method, the spatial three-dimensional coordinates of alpha-carbon atoms of the amino acids of the individual helices that make up the superhelix are used as input data for the chirality determination. This assumption allows each individual element of the secondary structure of a protein

(α-helix or collagen helix) to be considered as an unbranched consecutive chain of points, and this interpretation of individual helices is the basis for the proposed method.

We suppose it is natural to estimate the degree of superhelix chirality as the value showing how intensively each individual helix is twisted in relation to the superhelix axis characterizing the whole structure at the higher hierarchical level.

Before describing the method, we introduce an auxiliary definition. We call the center of some set of points such a point, each coordinate of which is obtained as the arithmetic mean of the corresponding coordinates of all points in the set. Thus, for a set of points A, B, and C, the coordinates of the center O will be calculated with the following formulas:

$$O_x = \frac{A_x + B_x + C_x}{3}; O_y = \frac{A_y + B_y + C_y}{3}; O_z = \frac{A_z + B_z + C_z}{3}. \quad (1)$$

Let us consider the steps for determining the chirality of a superhelix in our method, using as example the superhelix from a protein with PDB ID 1MG1 [37] (Figure 1a). As the method uses spatial coordinates of amino acid alpha carbons only, a carbon backbone remains from the protein chain, and the reference points are constructed from the alpha carbon's coordinates (Figure 1b). Because each amino acid residue is represented by only one point, it is indifferent where the N-terminus or C-terminus is located. In the first step, the superhelix axis is constructed. In our method, we approximate the superhelix axis with a straight line. To do this, we construct the centers of the terminal alpha carbons of all the helices composing the superhelix at one end (center of points C_1^1, C_1^2, C_1^3—point A_1), and then at the other (center of points C_n^1, C_n^2, C_n^3—point A_2). A line is drawn through these two points, which, according to our method, is the axis of the superhelix (Figure 1c).

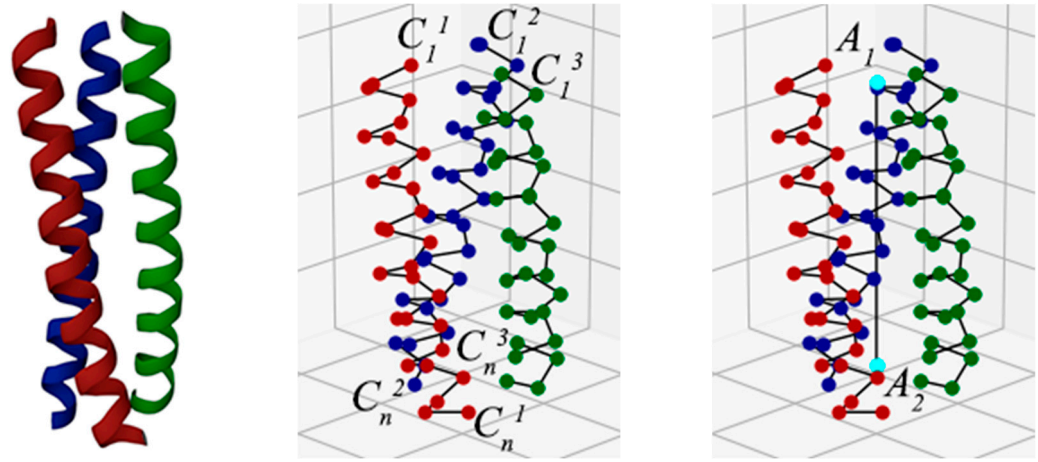

(**a**) (**b**) (**c**)

Figure 1. The first step of the method using protein superhelix (PDB ID 1MG1) as an example [37]: (**a**) Cartoon representation of superhelix. (**b**) Superhelix represented as alpha-carbon chains. The points C_1^1, C_1^2, C_1^3, C_n^1, C_n^2, C_n^3 are the end reference points for the three helices. Because every amino acid residue is represented by only one point, it is indifferent where the N-terminal or C-terminal end is located. (**c**) Superhelix with axis through points A_1 and A_2, which are the centers of points C_1^1, C_1^2, C_1^3 and points C_n^1, C_n^2, C_n^3, respectively. At further stages, these points are used to construct the axis of the superhelix.

Then we work with each helix of the superhelix separately. In the second step, we construct the centers of the first and last turns of the helices that make up the superhelix. Because the α-helix in the coiled-coil has approximately 3.5 amino acid residues per turn [16], the center of the first and last turns is taken as the center of the first four (C_1, C_2, C_3, and C_4) and the last four (C_{n-3}, C_{n-2}, C_{n-1}, and C_n) consecutive helix anchor points (Figure 2a). After this, a perpendicular is drawn from the centers of these turns to the axis of the superhelix, and from the intersection point of the perpendicular with the axis, a

vector to the center of the turn is constructed (Figure 2b). Let us call the vector to the center of the first turn $\mathbf{v_1}$ and the vector to the center of the last turn $\mathbf{v_2}$. The angle between $\mathbf{v_1}$ and $\mathbf{v_2}$ characterizes the helix twist around the superhelix axis (Figure 3).

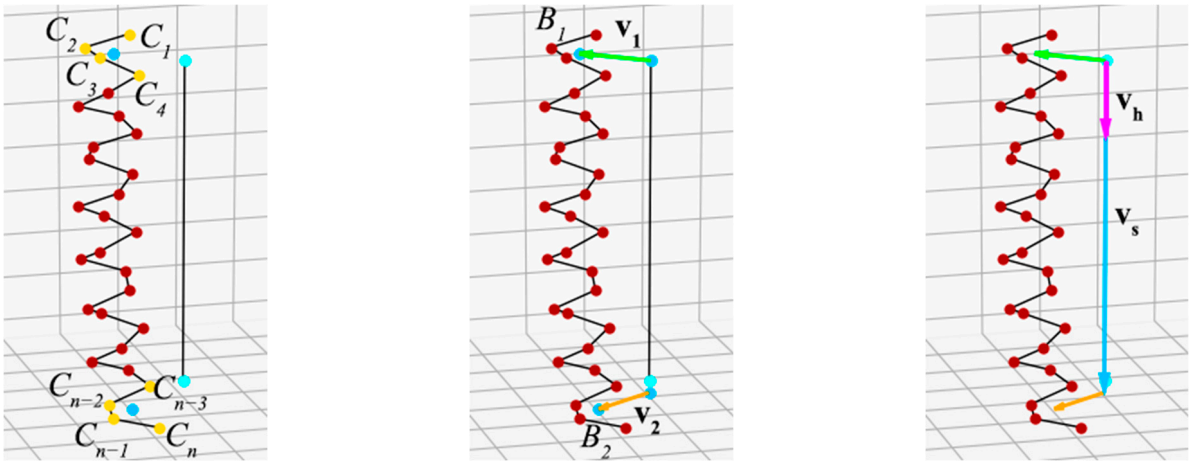

(**a**) (**b**) (**c**)

Figure 2. Construction of vectors for a single helix: (**a**) The center of the first turn is constructed as the center of the first four points of the helix, and the center of the last turn is constructed as the center of the last four points of the helix. (**b**) Vectors $\mathbf{v_1}$ and $\mathbf{v_2}$ perpendicular to the axes are constructed from the axis to the centers of the turns. (**c**) Construction of vectors to determine the chirality sign of the superhelix. $\mathbf{v_h}$ is the vector product of $\mathbf{v_1}$ and $\mathbf{v_2}$; $\mathbf{v_s}$ is a vector constructed along the axis of the superhelix.

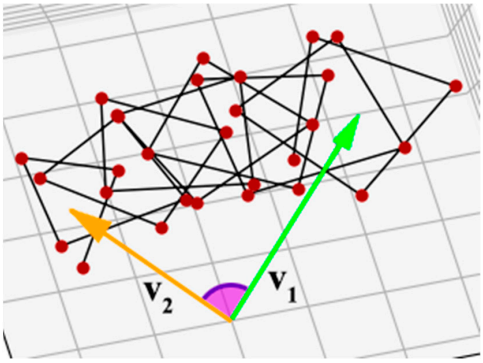

Figure 3. The third step of the method. The angle between the vectors $\mathbf{v_1}$ and $\mathbf{v_2}$ characterizes the twist of the helix around the axis.

An individual helix can twist around the axis to the right or to the left, and this determines the chirality sign of the superhelix. To calculate the twist direction, we propose to use a mixed vector product. Let $\mathbf{v_h}$ be the vector resulting from the vector product of $\mathbf{v_1}$ and $\mathbf{v_2}$, and $\mathbf{v_s}$ be the vector constructed along the axis of the superhelix. Vectors $\mathbf{v_s}$ and $\mathbf{v_h}$ are directed along the same line. If the superhelix is left-handed, the angle between the vectors $\mathbf{v_s}$ and $\mathbf{v_h}$ will be 0° (Figure 2c); if the superhelix is right-handed, this angle will be 180°. Thus, the sign of the scalar product of vectors $\mathbf{v_s}$ and $\mathbf{v_h}$ indicates the direction of the helix twist. Because the scalar product of two arbitrary vectors is given by the formula:

$$\mathbf{v_a} \cdot \mathbf{v_b} = x_a x_b + y_a y_b + z_a z_b = |\mathbf{v_a}| \cdot |\mathbf{v_b}| \cdot \cos(\mathbf{v_a}, \mathbf{v_b}), \quad (2)$$

the result will have the same sign as the cosine of the angle between the vectors, i.e., positive for the left-handed superhelices and negative for the right-handed ones.

The angle between $\mathbf{v_1}$ and $\mathbf{v_2}$ characterizes the twist of the helix around the superhelix axis. It can also be calculated using the scalar product of vectors:

$$\angle(\mathbf{v_1}, \mathbf{v_2}) = \arccos(\mathbf{v_1} \cdot \mathbf{v_2} / (|\mathbf{v_1}| \cdot |\mathbf{v_2}|)). \quad (3)$$

However, the angle calculated in this way will always be less than or equal to 180°, which in many cases does not correctly represent the actual helix twist. For example, in a protein with PDB ID 1X8Y [38], the corresponding angle is greater than 180° (Figure 4). There are also superhelices in which the individual helices are twisted around the superhelix axis for one or more full turns, and the result of the calculation should reflect this fact. Therefore, the angle between the vectors must be evaluated taking into account how the helix is arranged in the gap between vectors $\mathbf{v_1}$ and $\mathbf{v_2}$.

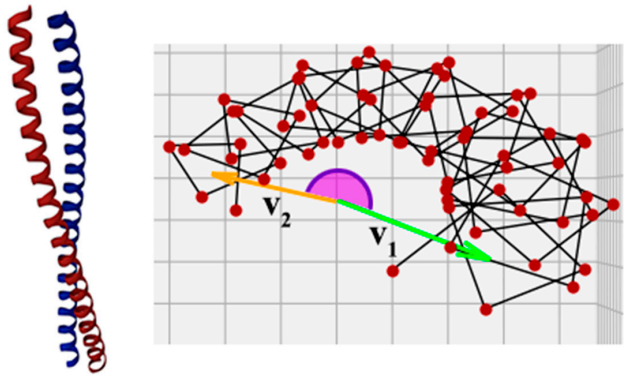

Figure 4. Superhelix from protein with PDB ID 1X8Y [38]. The angle between vectors $\mathbf{v_1}$ and $\mathbf{v_2}$ in this superhelix is greater than 180°, so it is impossible to determine the chirality degree properly using Formula (3).

In order to do this, we add intermediate steps to the calculation. We propose to sequentially calculate the corresponding angles between the vectors drawn to each of the two neighboring anchor points and sum all these angles, taking into account the direction of twist (Figure 5). Because each angle will be smaller than 180°, the result of the calculation according to Formula (3) will be correct. The total angle will characterize the helix twist around the axis. Further arithmetic averaging of the angles obtained for all the helices gives an effective angle for the whole superhelix. The sign of this number indicates the direction of the superhelix: negative numbers indicate a right-handed superhelix, and positive numbers indicate a left-handed one. Thus, the obtained effective angle with the sign serves as a final assessment of the degree of superhelix chirality in our method.

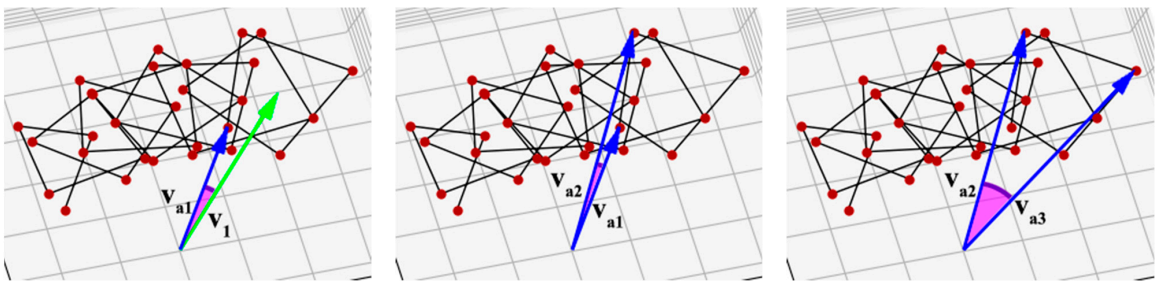

(**a**) (**b**) (**c**)

Figure 5. Sequential chirality calculation: $\mathbf{v_{a1}}$ is the vector from the superhelix axis to the first reference point, $\mathbf{v_{a2}}$ is to the second reference point, and $\mathbf{v_{a3}}$ is to the third reference point. (**a**) The angle between the vector to the first turn and the vector to the first reference point; (**b**) the angle between the vectors to the first and second reference points; (**c**) the angle between the vectors to the second and third reference points.

3. Results

The method was applied to calculate the chirality of 114 coiled-coil superhelices and 12 collagen superhelices. All the coiled-coil structures were left-handed and the collagen superhelices were right-handed. This result provides formal support for the hypothesis that the chirality sign in protein structures changes during the transition between hierarchical levels: right-handed α-helices produce left-handed coiled-coil superhelices, and left-handed collagen chains produce right-handed superhelices.

The mathematical interpretation of the method does not imply any specific format for recording the raw data. However, technically, we take the data of the real structures from the PDB [39] and information about which amino acid residues are included in the superhelix from the CC+ Database [40].

The raw data for the processed superhelices and the results of the calculations are presented in Table S1. The calculation results are also shown graphically in Figure 6, where the dots indicate the location of the superhelix in a two-coordinate system: the abscissa axis represents the number of amino acid residues in individual superhelices, while the ordinate axis represents our estimate of chirality for a given structure.

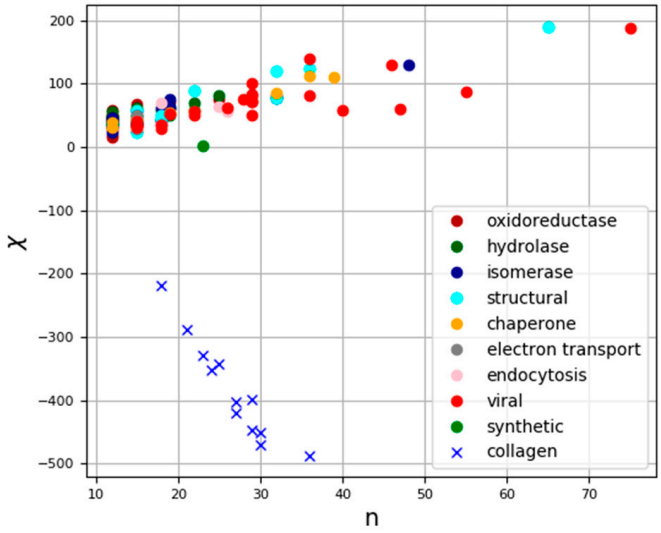

Figure 6. Graphical representation of chirality of superhelices for all calculated structures. Abscissa axis shows chiral length of corresponding structure in amino acid residues, ordinate axis shows numerical value of chirality.

4. Discussion

The degree of chirality of the superhelix in our method characterizes the twist of each individual helix around the superhelix axis; i.e., it is directly related to the number of turns each helix makes around the axis. The chirality degree of the collagen superhelices was significantly higher than that of the coiled-coil superhelices per number of amino acid residues in the helices, indicating that collagen superhelices are much more twisted around their axes.

According to our method, the chirality of superhelices does not depend linearly on the lengths of the constituent α-helices in the amino acid residues. Thus, coiled-coil helices of the proteins 1WU9 [41] and 1IO1 [42] have the same length (32 amino acid residues), but the degree of their chirality differs by more than one and a half times (120.8 and 76.9, respectively). At the same time, the helices of the coiled-coil proteins 1IO1 and 2NOV [43] have different lengths (32 and 19 amino acid residues, respectively), but their degrees of chirality are almost the same (76.9 and 76.4, respectively) (Figure 7).

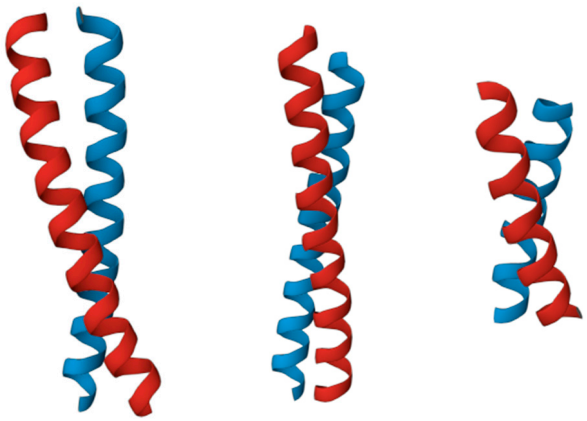

(**a**) (**b**) (**c**)

Figure 7. Superhelices with different lengths and chirality: (**a**) A superhelix from a protein with PDB ID 1WU9. The length of the helices is 32 amino acid residues. The chirality of the structure is 120.8. (**b**) A superhelix from a protein with PDB ID 1IO1. The length of the helices is 32 amino acid residues. The chirality of the structure is 76.9. (**c**) A superhelix from a protein with PDB ID 2NOV. The length of the helices is 19 amino acid residues. The chirality of the structure is 76.4.

5. Conclusions

The proposed method makes it possible to calculate not only the sign but also the degree of chirality. An important advantage of this method is the possibility of evaluating not only superhelices with classical heptadic repeats, but also those with different heptadic disruptions. We presently consider the superhelix axis as a straight line plotted on two points. In the future, we hope to improve the model so that the superhelix axis fully reflects all the bends and local features of the real structure. The presented method as well as the previously developed method for quantitative analysis of the chirality of helical structures [12,36] are stages in the development of methods for estimating the chirality of protein globules.

The chirality degree of the structure allows one to estimate and compare the curvatures of different superhelices with each other. It is one of the important and most obvious manifestations of physical principles in the formation of superhelical structures. It may help in elucidating the physical interactions within proteins that lead to the formation of a particular structure and in understanding the mechanisms of their functioning. Therefore, further research should be carried out to elucidate both the effect of this factor on the biochemical and other functional features of proteins and the possibility of altering the degree of chirality of the superhelix to obtain the desired properties. The degree of chirality could be an important marker for superhelices, allowing a comprehensive and effective assessment of their structural characteristics. This could be useful, for example, for pharmacology, in the development of drugs that have superhelices in their structures and for therapeutic effects on target superhelices.

Supplementary Materials: The following supporting information can be downloaded at: https://www.mdpi.com/article/10.3390/sym15112051/s1, Table S1. Table with computational data for all calculated helices.

Author Contributions: Conceptualization, A.S., A.L. and D.S.; methodology, A.L., A.S. and D.S.; software, A.L. and D.S.; investigation, A.L.; writing—original draft, A.L., A.S. and D.S.; writing—review and editing, E.B.; visualization, A.L.; supervision, A.S. and V.T. All authors have read and agreed to the published version of the manuscript.

Funding: The research was carried out with the financial support of the Foundation for the Development of Theoretical Physics and Mathematics "BASIS" within project no. 23-2-10-25-1 (to Aleksey Lutsenko) and project no. 23-2-10-8-1 (to Denis Shpigun).

Data Availability Statement: Publicly available datasets were analyzed in this study. This data can be found here: http://www.rcsb.org (accessed on 5 May 2023); http://coiledcoils.chm.bris.ac.uk/ccplus/search/ (accessed on 5 May 2023).

Conflicts of Interest: The authors declare no conflict of interest.

References

1. Mezey, P. Chirality Measures and Graph Representations. *Comput. Math. Appl.* **1997**, *34*, 105–112. [CrossRef]
2. Petitjean, M. Chirality and Symmetry Measures: A Transdisciplinary Review. *Entropy* **2003**, *5*, 271–312. [CrossRef]
3. Mezey, P.G. The proof of the metric properties of a fuzzy chirality measure of molecular electron density clouds. *J. Mol. Str. Theochem.* **1998**, *455*, 183–190. [CrossRef]
4. Luzanov, A.V.; Nerukh, D. Complexity and chirality indices for molecular informatics: Differential geometry approach. *Funct. Mater.* **2005**, *12*, 55–64.
5. Ramachandran, G.N.; Ramakrishnan, C.; Sasisekharan, V. Stereochemistry of polypeptide chain configurations. *J. Mol. Biol.* **1963**, *7*, 95–99. [CrossRef]
6. Baruch-Shpigler, Y.; Wang, H.; Tuvi-Arad, I.; Avnir, D. Chiral Ramachandran Plots I: Glycine. *Biochemistry* **2017**, *56*, 5635–5643. [CrossRef]
7. Zacharias, J.; Knapp, E.W. Geometry motivated alternative view on local protein backbone structures. *Protein Sci.* **2013**, *22*, 1669–1674. [CrossRef]
8. Neukirch, S.; Goriely, A.; Hausrath, A.C. Chirality of coiled coils: Elasticity matters. *Phys. Rev. Lett.* **2008**, *100*, 038105. [CrossRef]
9. Zheng, Y.; Mao, K.; Chen, S.; Zhu, H. Chirality Effects in Peptide Assembly Structures. *Front. Bioeng. Biotechnol.* **2021**, *9*, 703004. [CrossRef] [PubMed]
10. Petitjean, M. Extreme asymmetry and chirality—A challenging quantification. *Symmetry: Cult. Sci.* **2020**, *31*, 439–447. [CrossRef]
11. Wang, H.; Avnir, D.; Tuvi-Arad, I. Chiral Ramachandran Plots II: General trends and proteins chirality spectra. *Biochemistry* **2018**, *57*, 6395–6403. [CrossRef]
12. Sidorova, A.; Bystrov, V.; Lutsenko, A.; Shpigun, D.; Belova, E.; Likhachev, I. Quantitative Assessment of Chirality of Protein Secondary Structures and Phenylalanine Peptide Nanotubes. *Nanomaterials* **2021**, *11*, 3299. [CrossRef]
13. Tverdislov, V.A. Chirality as a Primary Switch of Hierarchical Levels in Molecular Biological Systems. *Biophysics* **2013**, *58*, 128–132. [CrossRef]
14. Tverdislov, V.A.; Malyshko, E.V. On regularities of spontaneous formation of structural hierarchies in chiral systems of non-living and living nature. *Phys. Usp.* **2019**, *62*, 354. [CrossRef]
15. Moutevelis, E.; Woolfson, D.N. A periodic table of coiled-coil protein structures. *J. Mol. Biol.* **2009**, *385*, 726–732. [CrossRef] [PubMed]
16. Lupas, A.N.; Gruber, M. The structure of α-helical coiled coils. *Adv. Prot. Chem.* **2005**, *70*, 37–78. [CrossRef]
17. Rose, A.; Meier, I. Scaffolds, levers, rods and springs: Diverse cellular functions of long coiled-coil proteins. *CMLS Cell. Mol. Life Sci.* **2004**, *61*, 1996–2009. [CrossRef] [PubMed]
18. Rackham, O.J.L.; Madera, M.; Armstrong, C.T.; Vincent, T.L.; Woolfson, D.N.; Gough, J. The evolution and structure prediction of coiled coils across all genomes. *J. Mol. Biol.* **2010**, *403*, 480–493. [CrossRef]
19. Ohtaki, A.; Kida, H.; Miyata, Y.; Ide, N.; Yonezawa, A.; Arakawa, T.; Iizuka, R.; Noguchi, K.; Kita, A.; Odaka, M.; et al. Structure and molecular dynamics simulation of archaeal prefoldin: The molecular mechanism for binding and recognition of nonnative substrate proteins. *J. Mol. Biol.* **2008**, *376*, 1130–1141. [CrossRef]
20. Perry, J.J.; Asaithamby, A.; Barnebey, A.; Kiamanesch, F.; Chen, D.J.; Han, S.; Tainer, J.A.; Yannone, S.M. Identification of a coiled coil in Werner syndrome protein that facilitates multimerization and promotes exonuclease processivity. *J. Biol. Chem.* **2010**, *285*, 25699–25707. [CrossRef]
21. Strauss, H.M.; Keller, S. Pharmacological interference with protein-protein interactions mediated by coiled-coil motifs. In *Protein–Protein Interactions as New Drug Targets*, 1st ed.; Klussmann, E., Scott, J., Eds.; Springer: Berlin/Heidelberg, Germany, 2008; pp. 461–482. [CrossRef]
22. McFarlane, A.A.; Orriss, G.L.; Stetefeld, J. The use of coiled-coil proteins in drug delivery systems. *Eur. J. Pharmacol.* **2009**, *625*, 101–107. [CrossRef] [PubMed]
23. Crick, F.H.C. The packing of α-helices: Simple coiled-coils. *Acta Crystallogr.* **1953**, *6*, 689–697. [CrossRef]
24. Walshaw, J.; Wooflson, D.N. Extended knobs-into holes packing in classical and complex coiled-coil assemblies. *J. Struct. Biol.* **2003**, *144*, 349–361. [CrossRef] [PubMed]
25. Mason, J.M.; Arndt, K.M. Coiled-coil domains: Stability, specificity and biological implications. *ChemBioChem* **2004**, *5*, 170–176. [CrossRef] [PubMed]
26. Brown, J.H.; Cohen, C.; Parry, D.A.D. Heptad breaks in α-helical coiled coils: Stutters and stammers. *Proteins* **1996**, *26*, 134–145. [CrossRef]
27. Hicks, M.R.; Holberton, D.V.; Kowalczyk, C.; Woolfson, D.N. Coiled-coil assembly by peptides with non-heptad sequence motifs. *Fold. Des.* **1997**, *2*, 149–158. [CrossRef] [PubMed]

28. Schmidt, N.W.; Grigoryan, G.; DeGrado, W.F. The accommodation index measures the perturbation associated with insertions and deletions in coiled-coils: Application to understand signaling in histidine kinases. *Protein Sci.* **2017**, *26*, 414–435. [CrossRef]
29. Shoulders, M.D.; Raines, R.T. Collagen Structure and Stability. *Annu. Rev. Biochem.* **2009**, *78*, 929–958. [CrossRef]
30. Ricard-Blum, S. The Collagen Family. *Cold Spring Harb. Perspect. Biol.* **2011**, *3*, a004978. [CrossRef]
31. Kaur, J.; Reinhardt, D.P. Extracellular Matrix (ECM) Molecules. In *Stem Cell Biology and Tissue Engineering in Dental Sciences*, 1st ed.; Vishwakarma, A., Sharpe, P., Songtao, S., Ramalingam, M., Eds.; Elseveir: London, UK, 2014; pp. 27–34.
32. Crick, F.H.C. The Fourier Transform of a Coiled-Coil. *Acta Crystallogr.* **1953**, *6*, 685–689. [CrossRef]
33. Offer, G.; Hicks, M.R.; Woolfson, D.N. Generalized Crick equations for modeling noncanonical coiled coils. *J. Struct. Biol.* **2002**, *137*, 41–53. [CrossRef]
34. Fraser, R.D.B.; MacRae, T.P. *Conformation in Fibrous Proteins and Related Synthetic Polypeptides*, 1st ed.; Academic Press: New York, NY, USA, 1973; p. 628.
35. Phillips, G.N. What Is the Pitch of the α-Helical Coiled Coil? *Proteins* **1992**, *14*, 425–429. [CrossRef]
36. Sidorova, A.E.; Malyshko, E.V.; Lutsenko, A.O.; Shpigun, D.K.; Bagrova, O.E. Protein helical structures: Defining handedness and localization features. *Symmetry* **2021**, *13*, 879. [CrossRef]
37. Kobe, B.; Center, R.J.; Kemp, B.E.; Poumbourios, P. Crystal structure of human T-cell leukemia virus type 1 gp21 ectodomain crystallized as a maltose-binding protein chimera reveals structural evolution of retroviral transmembrane proteins. *Proc. Natl. Acad. Sci. USA* **1999**, *96*, 4319–4324. [CrossRef] [PubMed]
38. Strelkov, S.V.; Schumacher, J.; Burkhard, P.; Aebi, U.; Herrmann, H. Crystal Structure of the Human Lamin A Coil 2B Dimer: Implications for the Head-to-tail Association of Nuclear Lamins. *J. Mol. Biol.* **2004**, *343*, 1067–1080. [CrossRef] [PubMed]
39. RCSB PDB. Available online: https://www.rcsb.org/ (accessed on 5 May 2023).
40. The CC+ Database. Available online: http://coiledcoils.chm.bris.ac.uk/ccplus/search/ (accessed on 5 May 2023).
41. Honnappa, S.; John, C.M.; Kostrewa, D.; Winkler, F.K.; Steinmetz, M.O. Structural insights into the EB1–APC interaction. *EMBO J.* **2005**, *24*, 261–269. [CrossRef]
42. Samatey, F.A.; Imada, K.; Nagashima, S.; Vonderviszt, F.; Kumasaka, T.; Yamamoto, M.; Namba, K. Structure of the bacterial flagellar protofilament and implications for a switch for supercoiling. *Nature* **2001**, *410*, 331–337. [CrossRef] [PubMed]
43. Laponogov, I.; Veselkov, D.A.; Sohi, M.K.; Pan, X.-S.; Achari, A.; Yang, C.; Sanderson, M.R. Breakage-Reunion Domain of *Streptococcus pneumoniae* Topoisomerase IV: Crystal Structure of a Gram-Positive Quinolone Target. *PLoS ONE* **2007**, *2*, e301. [CrossRef] [PubMed]